



# Magnetic supported activated carbon obtained from walnut shells for bisphenol-a uptake from aqueous solution

A. O. Uzosike<sup>1</sup> · E. A. Ofudje<sup>2</sup> · O. K. Akiode<sup>1</sup> · C. V. Ikenna<sup>3</sup> · A. I. Adeogun<sup>1</sup> · J. O. Akinyele<sup>4</sup> · M. A. Idowu<sup>1</sup>

Received: 7 July 2020 / Accepted: 21 June 2022 / Published online: 13 July 2022  
© The Author(s) 2022

## Abstract

This work investigated the usability of activated carbon walnut shell (ACWS) and magnetic activated carbon walnut shell (MACWS) for Bisphenol-A (BPA) elimination from aqueous solution. Fourier-transform infrared (FT-IR) and X-ray diffraction (XRD) were used to study the chemistry of the adsorbents. Batch sorption studies at different temperatures, contact time, adsorbent dosage, pH and varied Bisphenol-A concentrations were performed, while pseudo-first-order and pseudo-second-order kinetics models were deployed to investigate the kinetic data. Equilibrium parameters were computed using the Dubinin–Radushkevich, Freundlich, Temkin and Langmuir isotherms, while Box–Behnken design was used to optimize the adsorption factors. FT-IR report showed the existence of O–H, C=O, C–O and C=C stretches in both adsorbents and Fe–O in MACWS, while XRD revealed an amorphous morphology. BPA removal by ACWS and MACWS with correlation coefficient ( $R^2$ ) > 0.9 showed that the pseudo-first-order kinetic model was the most appropriate for explaining the kinetic data. Judging from the values of the maximum adsorption capacity (115.85 and 166.67 mg/g for ACWS and MACWS, respectively), it can be inferred that the Langmuir isotherm best describes the equilibrium results. Thermodynamic investigation showed the process of Bisphenol-A uptake to be spontaneous and endothermic with entropy change ( $\Delta S^\circ$ ) values of 0.033 and 0.039 kJ/mol for ACWS and MACWS, respectively. The data obtained from the kinetics, isotherm and equilibrium studies revealed that ACWS and MACWS adsorbents were effective for the treatment of Bisphenol-A.

**Keywords** Walnut shell · Activated carbon · Surface response · Bisphenol-A · Wastewater

## Introduction

The incorporation of Bisphenol-A otherwise known as 2, 2-bis (4-hydroxyphenyl propane) (BPA) as a monomeric unit and as an additive in polymer industry has come of age. BPA was first used on commercial scale to solidify plastics and in the preparation of epoxy resin found in the protective linings of infant-feeding bottles, food and beverage packs, tableware (plates and mugs), water bottles, sports equipment, storage

containers and compact disks (Pivnenko et al. 2015). BPA has been classified as a xenoestrogen which is composed of different groups of naturally occurring chemicals that imitate the property of estradiol which is the female sex hormone estrogen. According to available report, there is a link between the deterioration in male reproductive function and environmental exposure of xenoestrogens (Akande et al. 2013). Presently, as a result of the wide use of BPA in the production of food packaging materials and other reports associating BPA imitating the property of estradiol, there is serious disquiet about its safety in consumer products containers. When foods with very high or very low pH or foods at high temperature come into contact with plastic material, it often leads to leaching of BPA from the plastic material into the food matrix (vom Saal and Hughes 2006). The high consumption of BPA in the plastics industry has caused great concern and the possible adverse health effects, and research on the elimination of BPA from the environment is of immense significance.

✉ M. A. Idowu  
maidowu408@yahoo.com

<sup>1</sup> Department of Chemistry, Federal University of Agriculture, P.M.B. 2240, Abeokuta, Nigeria

<sup>2</sup> Department of Chemical Sciences, Mountain Top University, Prayer City, Ibafo, Nigeria

<sup>3</sup> CSIR-Central Electrochemical Research Institute (CECRI), Karaikudi, Tamil Nadu 630003, India

<sup>4</sup> Department of Civil Engineering, Federal University of Agriculture, P.M.B. 2240, Abeokuta, Nigeria

Activated carbon can be obtained from different kinds of carbon-containing materials via carbonization and pyrolysis using activating agent in case of chemical activation (Ofudje et al. 2020; Adeogun et al. 2018). The pore volume, surface area and the functional group present on the surface determine the sorption capacity of the adsorbent (Ahmedna et al. 2004). High volume of lignocellulosic by-products from walnut shells may present low-cost and renewable precursors for the production of granular activated carbons. This is because it is readily available, and moreover, it can produce significant amounts of by-products of agricultural wastes. Their transformation into useful materials such as activated carbon will add value to these by-products of agricultural wastes, thereby diminishing the costs of waste disposal and providing alternative substitute to the commercial adsorbents obtained from nonrenewable sources (Ahmedna et al. 2004).

In water treatment technology, the use of magnetic filtration has emerged as one of the promising methods because it can provide rapid and efficient pollutant elimination from wastewater. Inexpensive but efficient activated carbon adsorbents which can bind to pollutants can be prepared and can then be separated magnetically. A magnetic separator can easily be used to separate the activated carbon adsorbents from solution even at a significant concentration of solids. This study effectively recycled walnut shells into inexpensive activated carbon (ACWS) and magnetic carbon (MACWS) which were subsequently utilized for BPA removal. Factors such as the effect of pH, duration time, adsorbent dosage and initial concentration of BPA on the uptake process were investigated. The study also evaluated the thermodynamic parameters, while the adsorption data were modeled using various isotherms and kinetic models. Statistically, the adsorption data were optimized using response surface model.

## Materials and methods

### Reagents and equipment

The sodium hydroxide (99%), phosphoric acid (99%), Bisphenol-A (99%), methanol (98%) and ferrous sulfate (99.5%) were obtained from Chemie Ltd. Distilled water was used throughout the study. The preparation of stock solution of BPA ( $\approx 200$  mg/L) was made using distilled water. A UV-visible spectrophotometer (PerkinElmer Lambda) was used to measure the concentration of BPA.

### Preparation of activated walnut shells

Washing of the walnut shells was done with tap water to eliminate contaminants and thereafter crushed so as to

separate the edible part from the shell. The shells were air-dried and soaked in 0.1 M  $\text{H}_3\text{PO}_4$  acid for 24 h for chemical activation followed by rinsing with distilled water. The drained shells were carbonized at a temperature of 500 °C in a furnace and thereafter pulverized and sieved. The walnut shell-derived activated carbon was referred to as ACWS and was then preserved for subsequent study.

### Development of magnetic activated carbon

Exactly 20 g of  $\text{FeSO}_4$  was dissolved in 150 cm<sup>3</sup> of distilled water, while a freshly prepared ferric chloride solution was made by dissolving 18 g of  $\text{FeCl}_3$  in 1300 cm<sup>3</sup> distilled water. The prepared ferrous sulfate and ferric chloride solution were vigorously stirred together at a temperature of 70 °C. 50 g of the ACWS was weighed and suspended into this mixture and slowly stirred together for 30 min at room temperature. The solution pH was raised to 11 following the drop-wise addition of 10 M NaOH solution to the mixture. The mixing was left to age for 24 h at room temperature, after which the content was separated and washed thoroughly with distilled water followed by ethanol. Thereafter, the sample was dried overnight at 80 °C in a hot air oven. The magnetic activated carbon as obtained from walnut shell was referred to as MACWS and preserved in an air tight container ready for use.

### Characterization of the prepared adsorbents

Functional groups available on the surface of the two adsorbents before and after the adsorption of BPA were investigated using Fourier-transform infrared spectroscopy (FT-IR). Measurements were done with the aid of KBr technique using a model 8400S (Shimadzu, Japan) at room temperature. The recording was done over the range of wavelength of 400–4000 cm<sup>-1</sup>. The X-ray diffraction (XRD) measurements were performed using PANalytical (X'Pert Pro, Netherlands) using Cu K $\alpha$  ( $\gamma = 1.54178$  Å) radiation at room temperature. The zeta potential of the ACWS and MACWS was carried out using 0.1 g of the sorbent in 15 cm<sup>3</sup> of Bisphenol-A solution. The pH adjustment was achieved using 0.1 M HCl or NaOH, and a Zetasizer Nano ZS instrument (Malvern, UK) was used to analyze the zeta potential of the adsorbents.

### Sorption procedure using ACWS and MACWS

To generate kinetics and equilibrium data, series of batch experiments were performed under different experimental conditions such as solution temperature, pH, adsorbent dosage, initial BPA concentration and duration time. The BPA sorption experiments were conducted within the range of 25–200 mg/L of BPA concentration. In a conical flask, 0.1 g of the adsorbent was dispersed into 25 cm<sup>3</sup> of BPA solution and agitated for a

maximum time of 140 min. The adsorbent was separated from the solutions and the absorbance was taken at a wavelength of 276 nm while the amount of BPA adsorbed was estimated using Eq. 1:

$$q_e = \frac{C_o - C_e}{m} \times V \tag{1}$$

where  $q_e$  is the quantity (mg/g) of BPA adsorbed,  $C_o$  and  $C_e$  are the concentrations (mg/L) of BPA at the beginning and final stage of the reaction process,  $V$  stands for the volume of BPA used in L, and  $m$  is the weight (g) of ACWS or MACWS used. To evaluate the role of contact time on the adsorption of BPA by the adsorbents, predetermined amounts of adsorbent were employed in the sorption process and agitated for preset time intervals until 140 min, and the percentage removal was estimated by using Eq. 2:

$$RE = \frac{C_o - C_e}{C_o} \times 100 \tag{2}$$

### Surface response evaluation by box–behnken design

The relationship that exists between the experimental outputs or responses and the various factors affecting it which are referred to as  $X_1, X_2, X_3, X_4$ , etc., can be explained using the surface response methodology as an empirical optimization technique. The number of experimental sets can be substantially reduced by adopting Box–Behnken designs without affecting the accuracy of the optimization. Symbol codes such as coded and uncoded terms were used to illustrate the minimum and maximum ranges of the four factors tested as illustrated in Table 1. The relationships between the coded and uncoded variables were obtained following the modified method Eqs. 3–6 described by Qiu et al. (2014):

$$x_1 = ((X_1 - 7))/5 \tag{3}$$

$$x_2 = ((X_2 - 47.5))/17.5 \tag{4}$$

$$x_3 = ((X_3 - 112.5))/87.5 \tag{5}$$

$$x_4 = ((X_4 - 465))/435 \tag{6}$$

where the uncoded variables are given as  $X_1, X_2, X_3$  and  $X_4$ , while  $x_1, x_2, x_3$  and  $x_4$  are the coded variables. A quadratic model was used to explain the impacts of these four variables on the removal efficiency ( $Y$ ) of BPA using Eq. 7 (Qiu et al. 2014):

$$Y = x_1 + x_2 + x_3 + x_4 + x_1^2 + x_2^2 + x_3^2 + x_4^2 + x_1x_2 + x_2x_3 + x_3x_4 + x_1x_4 \tag{7}$$

where  $x_1, x_2, x_3$  and  $x_4$  are pH, temperature, concentration and dosage, respectively (Gbasemian et al. 2013), and  $Y$  is the percentage removal efficiency which denotes the dependent variable and is given as Eq. 8 (Manzato et al. 2018):

$$Y = \frac{C_o - C_e}{C_o} \times 100 \tag{8}$$

where  $C_o$  and  $C_e$  are as previously defined.

## Results and discussion

### Characterizations

Powder X-ray diffraction patterns for ACWS and MACWS are presented in Fig. 1. A broad peak was observed at about  $2\theta \approx 25^\circ$  in ACWS authenticating the amorphous nature of the prepared carbon. On the other hand, the XRD patterns of MACWS display several sharp peaks ( $2\theta = 35.69, 43.11, 57.5$  and  $63.2^\circ$ ) which indicate the presence of Fe. Similar X-ray powder pattern was confirmed by Mohan and his group (Mohan et al. 2011). These iron contents were introduced during the preparation of MACWS. There were slight shifts in the positions of the peaks following adsorption of BPA, possibly due to interaction of the BPA with the adsorbents.

The FT-IR spectra of ACWS and MACWS before and after adsorption with BPA are listed in Fig. 2. Bisphenol-A FT-IR chart shows strong and broad band below  $3500\text{ cm}^{-1}$  displaying the existence of phenolic compound and peak at  $3000\text{ cm}^{-1}$  which indicates C-H stretch in aromatic compound (phenol), while the peak around  $1600\text{ cm}^{-1}$  signifies C–C stretch (in-ring) of aromatic compound. In ACWS, different functional groups were observed with peaks ranging from  $1750$  to  $1735\text{ cm}^{-1}$  indicating carbonyl (C=O stretch) in esters and saturated aliphatic compound. Activated walnut shell with BPA shows disappearance of phenolic functional group with peak indicating the formation of C=O stretch (carbonyl compound) in the range of  $1750$  to  $1735\text{ cm}^{-1}$ .

**Table 1** Minimum and maximum levels of coded and uncoded symbols of the four factors of BPA adsorption

Variables	Symbols		Level		
	Coded	Uncoded	-1	0	1
pH	$x_1$	$X_1$	2	7	12
Temperature (°C)	$x_2$	$X_2$	30	47.5	65
Dosage (mg)	$x_3$	$X_3$	30	465	900
Concentration (mg/L)	$x_4$	$X_4$	25	112.5	200

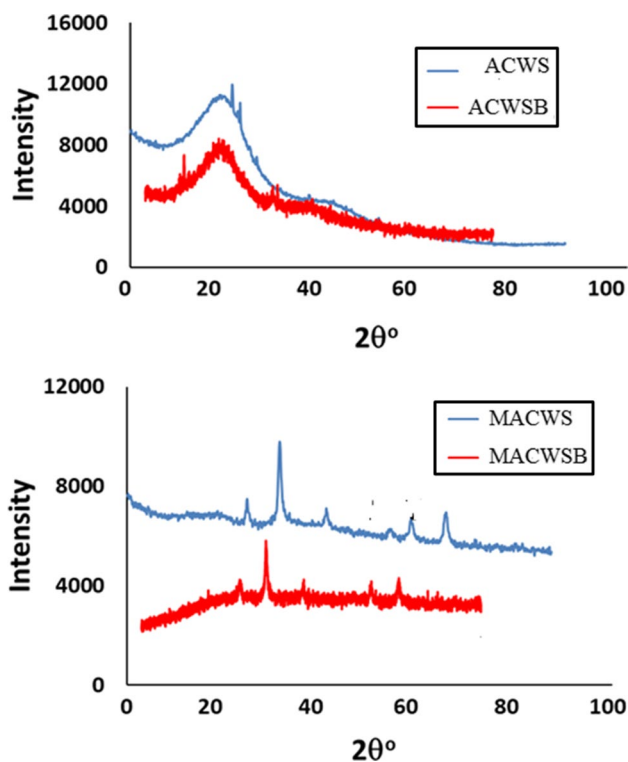
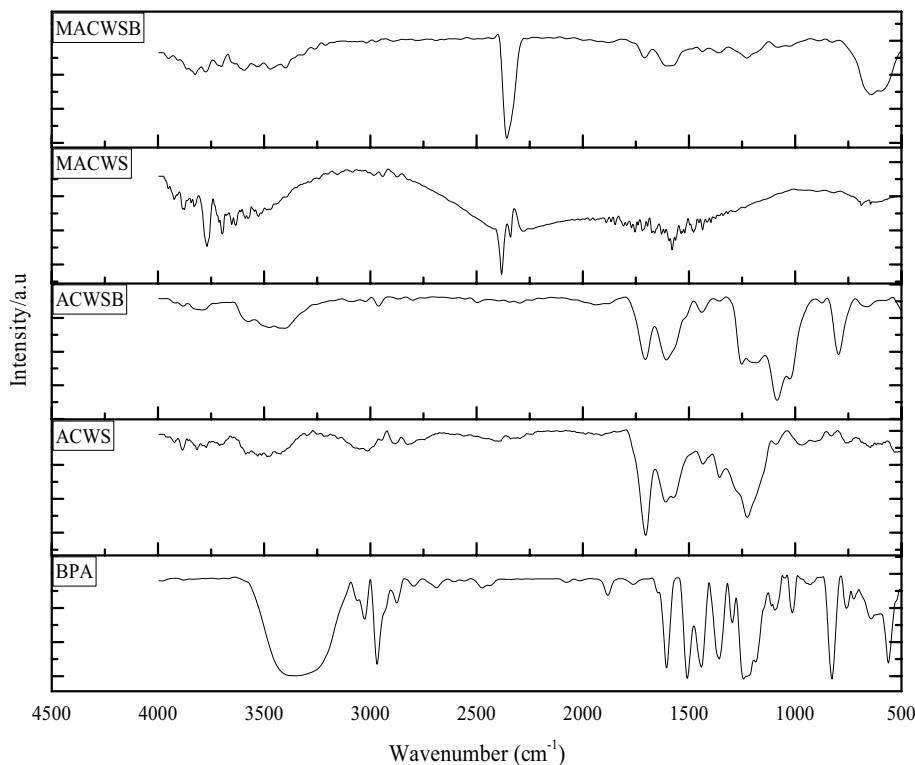


**Fig. 1** XRD spectra of ACWS and MACWS in the presence and absence of BPA

**Fig. 2** FT-IR spectra of ACWS and MACWS in the presence and absence of BPA

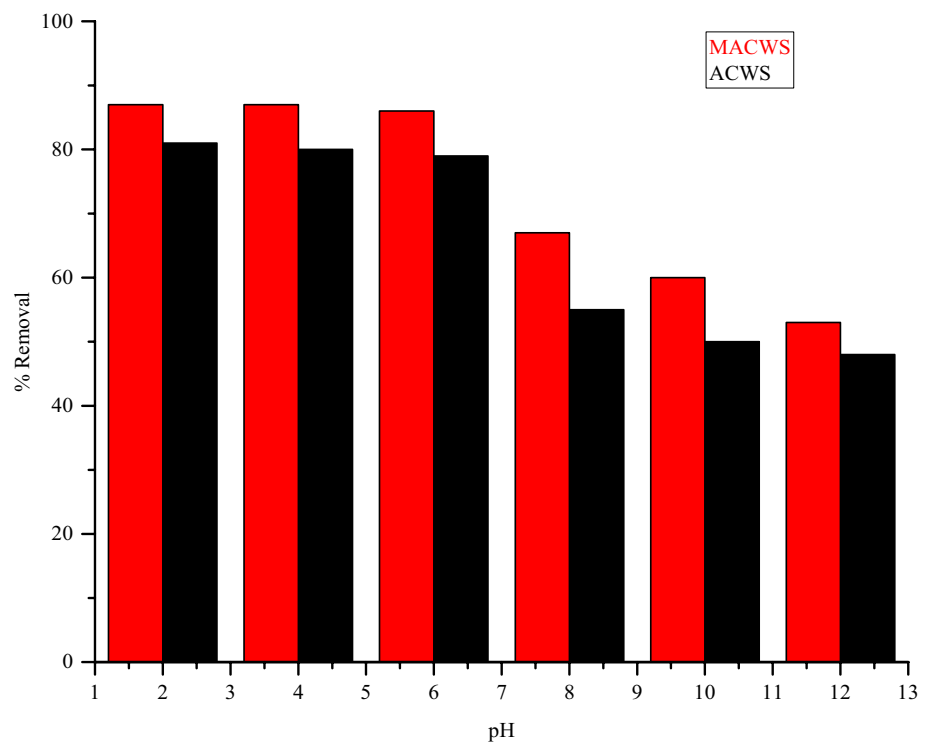


FT-IR of MACWS indicates O–H stretch above  $3500\text{ cm}^{-1}$ , while the peak around  $1700\text{ cm}^{-1}$  indicates C=O stretch. MACWSB shows weak peak around  $3500\text{ cm}^{-1}$  indicating disappearance of O–H group. The strong peak around  $2500\text{ cm}^{-1}$  indicates formation of O–H from carboxylic acid, and broad band around  $700\text{ cm}^{-1}$  indicates C–H bond of aromatic compound. In general, the notable adsorption sites of all the adsorbents mentioned are C=O, O–H and OH group sites on the surface of the adsorbent.

### Sorption studies

Solution pH plays vital role in adsorption process because of its great sway effect on the chemistry of both the adsorbent and the pollutant. The variation of the percentage of BPA adsorbed by MACWS and ACWS at various alternate pH values (1–12) at  $27\text{ }^{\circ}\text{C}$  and initial BPA concentration of  $200\text{ mg/L}$  is listed in Fig. 3. From the result of the pH dependence, BPA percentage removal was established to be relatively stable across low pH range but decreases at a pH greater than 7. BPA percentage removal was stable at around 81.0 to 87.3% at the initial solution pH range of 2 to 7 for both ACWS and MACWS adsorbents. This happening can be explained that BPA mainly existed in a neutral molecular form of BPA at  $\text{pH} < \text{pK}_a$  value which becomes deprotonated at pH higher than 8.0, thus forming mono- or divalent anions. This implies that the decrease in the removal percentage of BPA within the alkaline pH range might be

**Fig. 3** The role of pH on the removal of BPA by ACWS and MACWS at duration time of 100 min, BPA concentration of 200 mg/L, biomass dose of 0.09 g and temperature of 55 °C



as a result of the revolting electrostatic relation that exists between the surface of the adsorbents which is negatively charged and the bisphenolate anion. Related trend had also been reported in the literature (Zhou et al. 2016, 2018; Riry et al. 2014). The zero point charge of ACWS and MACWS obtained is 6.3 and 6.6, respectively, and beneath these values, the adsorbents surfaces are expected to be positively charged. This implies that for this study, BPA solution exists as anionic species which enhances its adsorption onto the surface of ACWS and MACWS within the acidic range. Since a pH above the zero point charge makes the surface of the biomass to become negatively charged, this explains why the uptake of BPA was hampered at alkaline pH range (Himanshu et al., 2010; Ofudje et al., 2017).

Also, the effect of adsorbents dosages (0.03 to 1 g) on the sorption of BPA was evaluated, while other parameters were kept constant. As shown in Fig. 4, the percentage of BPA removal at equilibrium for ACWS and MACWS increased from 64.10 to 75.84% and 73.90 to 79.48%, respectively, with increase in the adsorbents' dosage from 0.03 to 0.9 g. This result is supported by previous findings (Adeogun et al. (2018)), when it was found out that a rise in adsorbent dosage will lead to an increase in the amount of pollutant adsorbed which is due to increase in surface area of the adsorbent which accordingly increases the available receptor sites.

The results of the impacts of duration time (40 to 140 min) and initial adsorbate concentration (25 to 200 mg/L) for ACWS and MACWS are revealed in Figs. 5

and 6, respectively, which show that the reaction was quick at the early stage but reduces as the reaction approaches equilibrium. Ceiling uptake of BPA was achieved at a contact time of 100 min and BPA concentration of 200 mg/L. The amount of BPA adsorbed was established to rise from 4.32 to 10.33 mg/g for ACWS and from 10.23 to 14.80 mg/g for MACWS, respectively, when the duration time rose from 40 to 100 min at initial BPA concentration of 25 mg/L. Upon increasing the initial BPA concentration to 200 mg/L, the value of BPA adsorbed rose tremendously from 53.71 to 113.60 mg/g for ACWS and from 67.22 to 156.32 mg/g for MACWS, respectively.

The changes in the amount of adsorption with respect to time and BPA concentration might be due to the fact that at opening stage of the reaction, there were vacant absorber sites of the adsorbents coupled with high solute concentration which enhanced the process of adsorption; but, as the reaction proceeds, these vacant sites become filled up by the adsorbate particles, while the amount of the pollutant in the solution has been used up in the process, thus resulting in a decrease in the adsorption uptake as observed (Adeogun et al. 2018). According to Han et al. (2012a), longer time to get in touch with the adsorbate gives adequate duration time for the adsorption process to occur which enhances the adherence of the pollutant onto the receptor sites of the adsorbent. The results of the impact of temperature on the removal of BPA are shown in Fig. 7 which reveals that by increasing the temperature from 30 to 55 °C, the sorption capacity of BPA rose from 72.98%

**Fig. 4** The effect of dosage on the adsorption of BPA by ACWS and MACWS at contact time of 100 min, initial BPA concentration of 200 mg/L and temperature of 55 °C

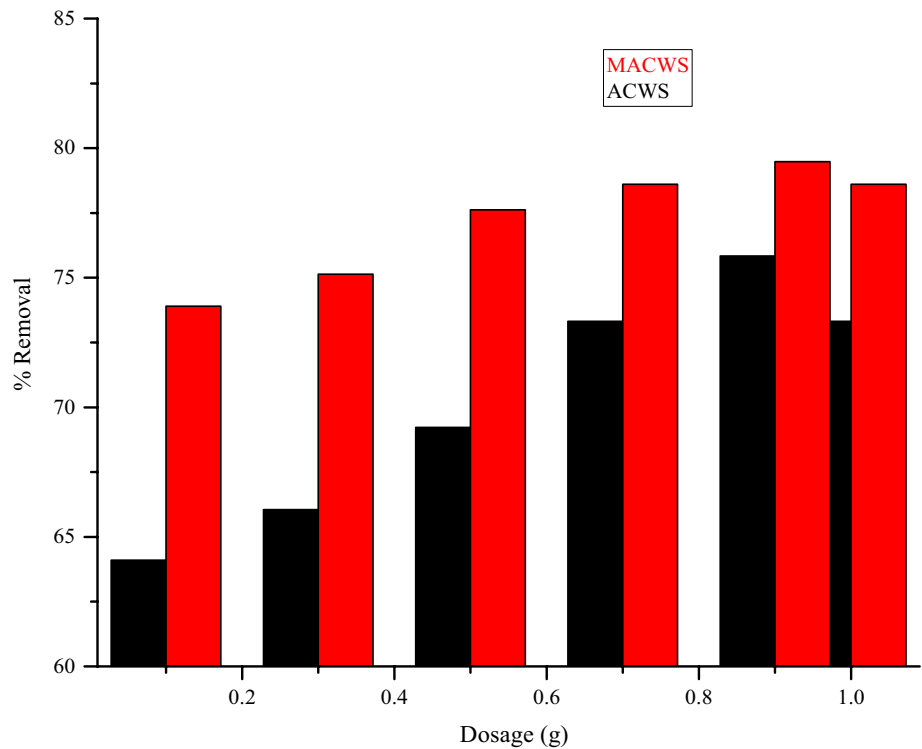
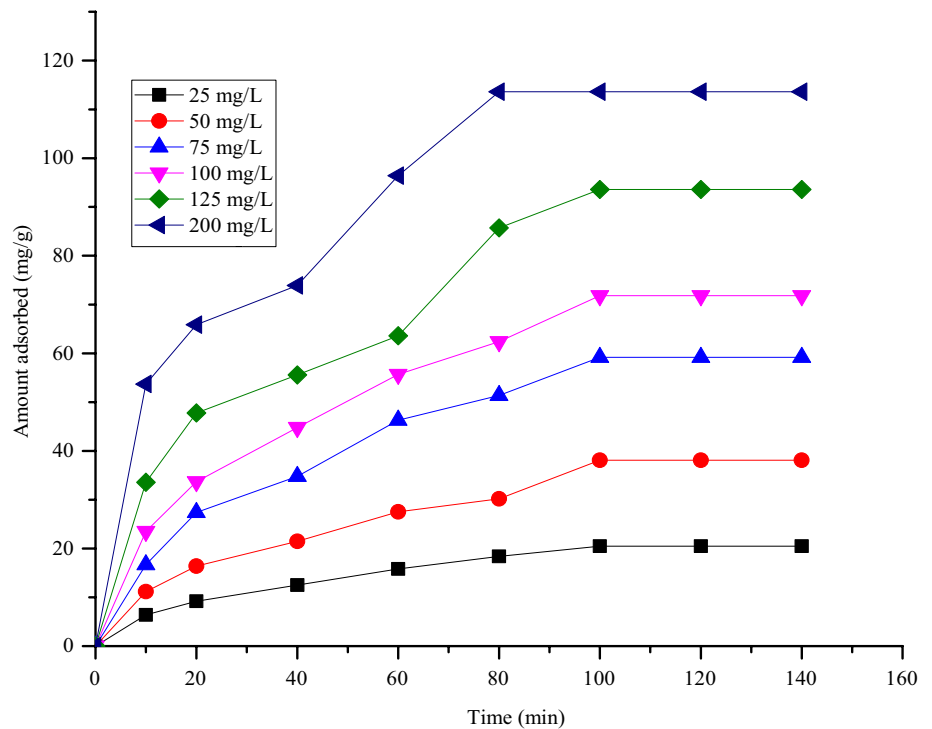


**Fig. 5** Impact of duration time and initial BPA concentrations on BPA uptake by ACWS at adsorbent dose of 0.09 g and temperature of 55 °C



to 78.57% and 73.16% to 81.70% for ACWS and MACWS, respectively. Beyond a temperature of 55 °C, there was no further major increase in the uptake of the BPA by the adsorbents and as such a temperature of 55 °C was selected for subsequent experiments. Literature reports

show that the rate of diffusion of the adsorbed molecules across the internal pores of the adsorbent particles as well as the external boundary layer can be enhanced by increase

**Fig. 6** Impact of duration time and initial BPA concentrations on BPA uptake by MACWS at adsorbent dose of 0.09 g and temperature of 55 °C

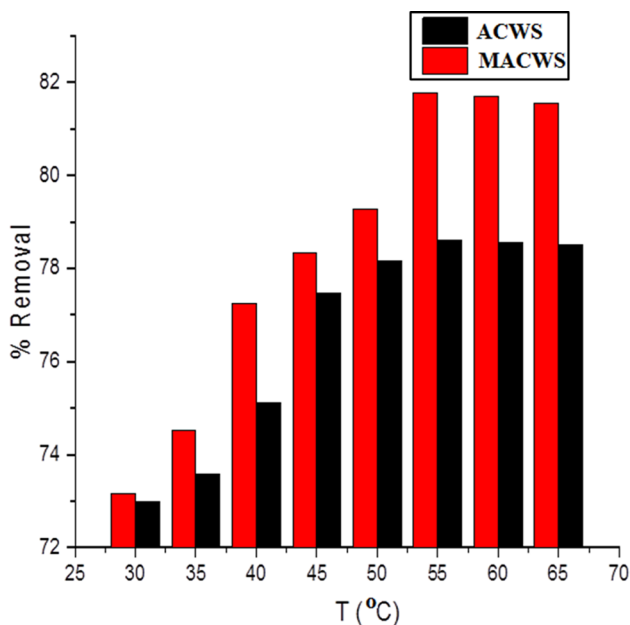
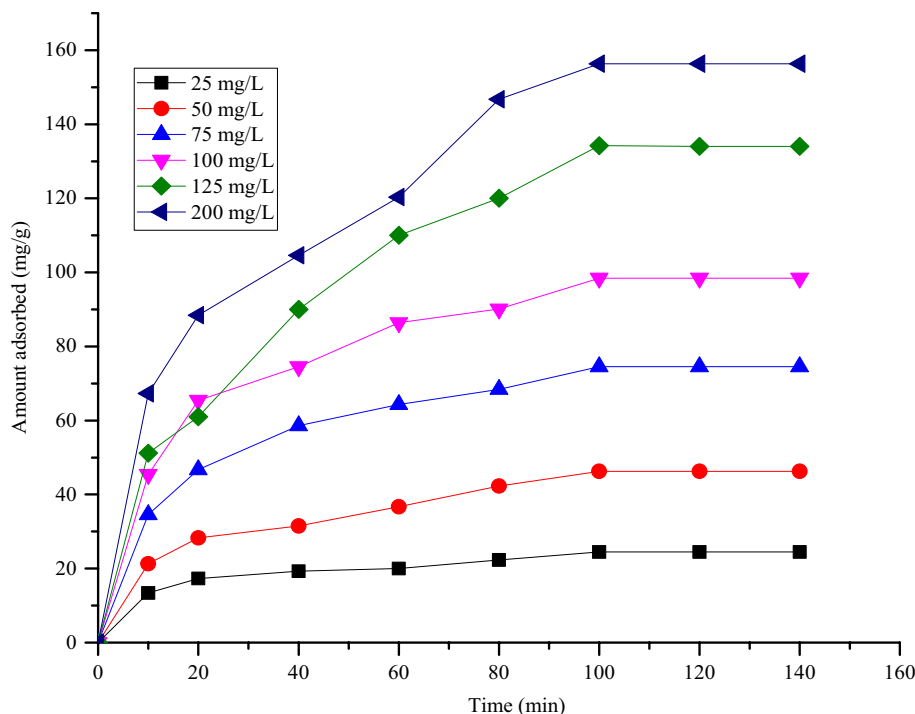


**Fig. 7** Effect of temperature on the adsorption of BPA at contact time of 100 min, initial BPA concentration of 200 mg/L and adsorbent dose of 0.09 g

in temperature of the adsorption process. The enhanced diffusion could be due to the decrease in the viscosity of the solution (Adeogun et al. 2011; Al-qodah 2000).

### Thermodynamic studies

The driving force of the adsorption process (Gibb’s free energy change) can be obtained from the equilibrium constant as described in Eq. 9 (Adeogun et al. 2011):

$$\Delta G^0 = -RT \ln K_c \tag{9}$$

where the equilibrium temperature is given as T in Kelvin, the ideal gas constant is denoted as R having value as 8.314 Jmol<sup>-1</sup> K<sup>-1</sup>, and the thermodynamic equilibrium constant is denoted as K<sub>c</sub>. The expression for the equilibrium constant can be obtained in Eq. 10:

$$K_c = C_a / C_e \tag{10}$$

where C<sub>a</sub> is the amount of adsorbate per liter and C<sub>e</sub> is as previously defined in mg/L. The enthalpy change (ΔH<sup>0</sup>), equilibrium constant as well as the entropy change (ΔS<sup>0</sup>) at constant temperature can be expressed using the Van’t Hoff equation (Eq. 11) as follows (Ofudje et al. 2020):

$$\ln K_c = \frac{\Delta S^0}{R} - \frac{\Delta H^0}{RT} \tag{11}$$

where the slope as well as the intercept of the Van’t Hoff plot of lnK<sub>c</sub> against 1/T as shown in Fig. 8 was used to estimate the values of enthalpy change (ΔH<sup>0</sup>) and entropy change (ΔS<sup>0</sup>) for the adsorption of BPA by ACWS and MACWS and their values are presented in Table 2. The endothermic nature of the adsorption process was confirmed by the positive values of ΔH<sup>0</sup>, while the randomness observed at the

**Fig. 8** Plot of  $\ln K_c$  against  $1/T$  for the adsorption of BPA by MACWS and ACWS

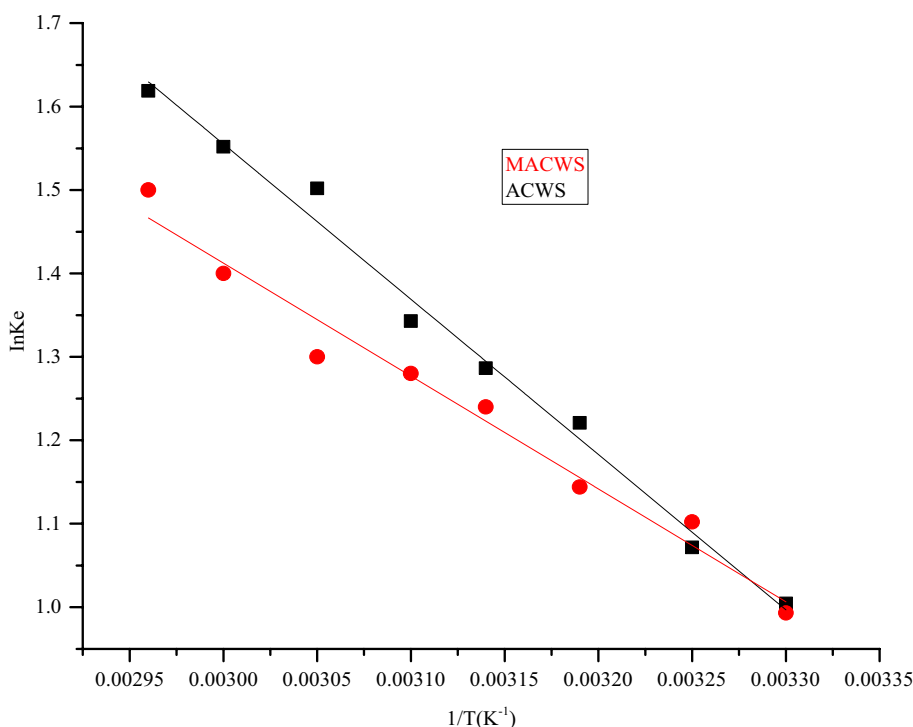


**Table 2** Thermodynamic parameters for the adsorption of BPA by ACWS and MACWS

Adsorbent	$\Delta H^\circ$ (kJ/mol)	$\Delta S^\circ$ (kJ/Kmol)	$T_1 =$ 303 K	$T_2 =$ 308 K	$T_3 =$ 313 K	$T_4 =$ 318 K	$T_5 =$ 323 K	$T_6 =$ 328 K	$T_7 =$ 333 K	$T_8 =$ 338 K
$\Delta G^\circ$ (kJ/mol)										
ACWS	9.17	0.039	-2.64	-2.84	-3.03	-3.23	-3.42	-3.62	-3.81	-4.01
MACWS	7.45	0.033	-2.55	-2.71	-2.88	-3.04	-3.21	-3.37	-3.54	-3.70

solid–solution interface in the course of the adsorption of BPA by ACWS and MACWS is substantiated from the positive values of  $\Delta S^\circ$  (Dang et al. 2009). The spontaneity of the adsorption can be ascertained from the Gibbs free energy change,  $\Delta G^\circ$ , and can be used to predict the feasibility of the process. Thus, the negative values obtained for  $\Delta G^\circ$  in the adsorption of BPA as listed in Table 2 substantiate the spontaneity as well as the feasibility of the adsorption process (Upendra 2011). Also, the  $\Delta G^\circ$  is seen to have increased as temperature increased for the two adsorbents used. A similar phenomenon was reported (Balci and Erkurt 2017) in the removal of BPA by Eucalyptus bark/magnet composite.

### Kinetic studies and modeling

Lagergren pseudo-first-order and Ho’s pseudo-second-order kinetic models were deployed as shown in the kinetic data plot in Fig. 9, while the values obtained from these plots are listed in Tables 3 and 4. The simple pseudo-first-order equation suggested by Lagergren is given as Eq. 12 (Ho 2004):

$$\text{Log}(q_e - q_t) = \text{log } q_e - \frac{k_1}{2.303}t \tag{12}$$

where the equilibrium concentration and the sorption capacity at time  $t$  are given as  $q_e$  and  $q_t$  in mg/g, respectively, and  $k_1$  is the rate constant of pseudo-first-order kinetic model. For pseudo-second-order kinetic model, the integrated form is given as Eq. 13 (Ho 2004):

$$\frac{t}{q_t} = \frac{1}{k_2 q_e^2} + \frac{1}{q_e} \tag{13}$$

where  $t$ =time,  $k_2$  is pseudo-second-order rate constant, and  $q_e$  and  $q_t$  are as previously defined. The values of  $q_e$  and those of  $k_1$  and  $k_2$  were computed using the least square plots as shown in Fig. 9. We observed that the theoretical values of  $q_e$  concur well with the values obtained for the experimental adsorption capacity from the pseudo-first-order model when compared with those of the pseudo-second-order kinetic model, although both models demonstrated high value of correlation coefficients and this is an indication of a physical adsorption process. Smaller values of sum of square



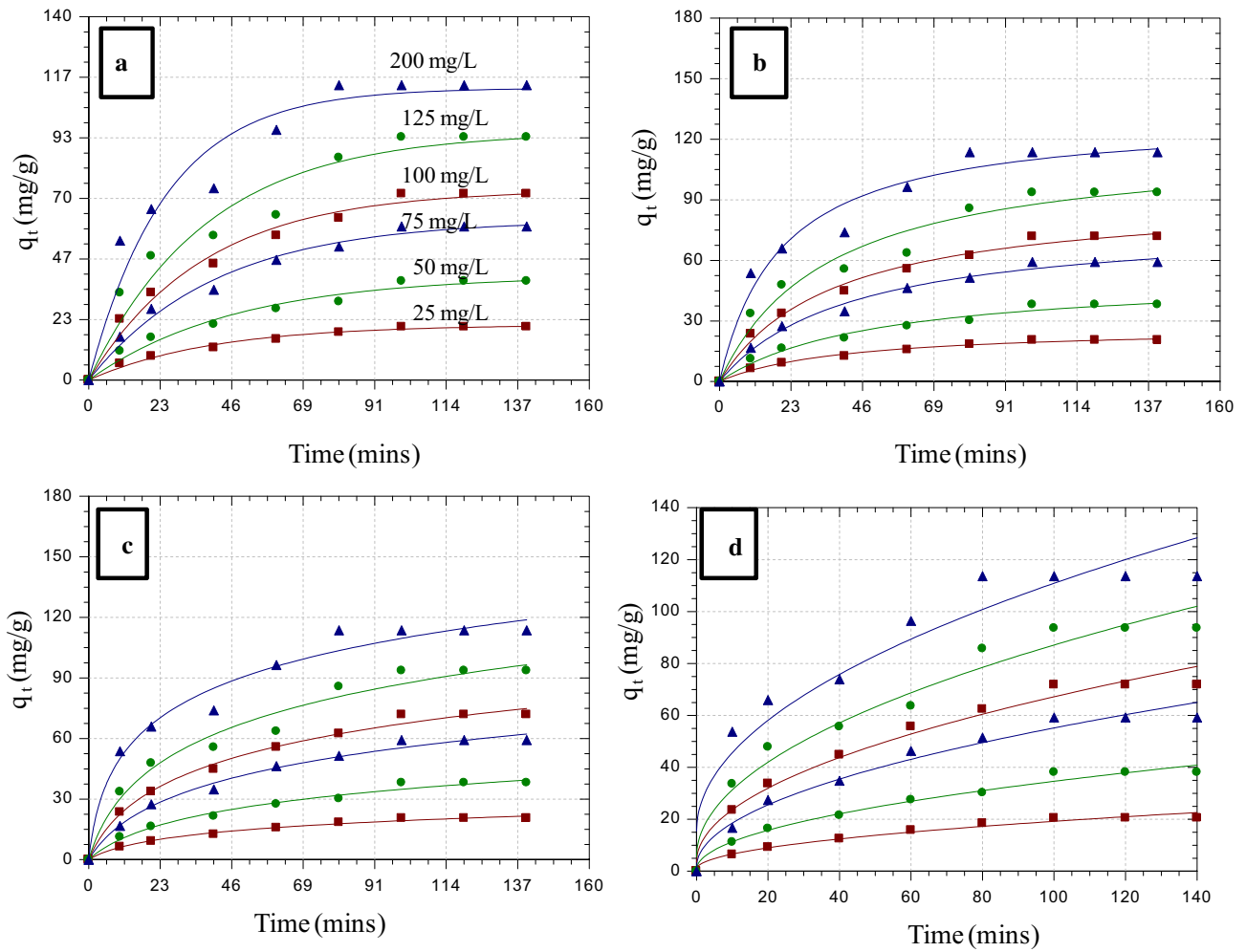


**Fig. 9** Graph of (a and c) pseudo-first-order and (b and d) pseudo-second-order kinetic models for the adsorption of BPA by ACWS and MACWS, respectively

**Table 3** Kinetics parameters for the adsorption of BPA by ACWS and MACWS

First order				Second order				
$q_e(\text{exp})$	$q_e(\text{cal})$	$k_1$	$R^2$	% SSE	$q_e(\text{cal})$	$k_2$	$R^2$	% SSE
<i>ACWS</i>								
20.520	21.288	0.009	0.983	0.158	27.112	0.004	0.981	0.527
38.113	40.262	0.033	0.998	0.001	52.449	0.023	0.992	0.076
59.143	61.659	0.011	0.994	0.037	79.155	0.005	0.994	0.185
71.857	73.334	0.023	0.996	0.008	92.096	0.007	0.997	0.097
93.602	95.475	0.048	0.998	0.009	118.156	0.014	0.999	0.031
113.625	112.519	0.020	0.994	0.026	131.397	0.001	0.995	0.169
<i>MACWS</i>								
22.331	22.960	0.014	0.974	0.022	25.738	0.002	0.93	0.367
42.302	44.474	0.013	0.959	0.006	55.861	0.003	0.93	0.216
68.426	71.989	0.017	0.989	0.030	82.883	0.004	0.996	0.128
90.105	94.757	0.034	0.997	0.004	108.737	0.007	0.999	0.114
134.221	135.335	0.053	0.997	0.012	166.516	0.016	0.999	0.032
146.704	153.287	0.020	0.995	0.027	181.447	0.001	0.998	0.148

**Table 4** Isotherm parameters for the adsorption of BPA onto ACWS and MACWS

Adsorbents						
Langmuir isotherm						
	$q_{\max}$ (mg/g)	$K_L$ (L/mg)	$R_L$	$R^2$	HYBRID	RMSE
ACWS	115.85	0.0096	0.26	0.963	0.034	0.320
MACWS	166.67	0.0030	0.38	0.984	0.027	0.121
Freundlich isotherm						
	1/n	n	$K_F$ (mg/g)	$R^2$	HYBRID	RMSE
ACWS	0.221	4.52	7.193	0.957	1.563	3.112
MACWS	0.877	1.14	8.306	0.965	1.890	4.220
Temkin isotherm						
	$\alpha T$ (L/mg)	$b_T$ (J/mol)	$R^2$	HYBRID	RMSE	
ACWS	2.397	345.53	0.929	0.933	2.224	
MACWS	2.117	336.58	0.942	0.484	2.807	
Dubinin–Radushkevich isotherm						
	$q_s$ (mg/g)	$K_{ad}$ (mol <sup>2</sup> /kJ <sup>2</sup> )	$E$ (kJ/mol)	$R^2$	HYBRID	RMSE
ACWS	10.585	$4 \times 10^{-5}$	0.112	0.998	0.260	3.108
MACWS	12.613	$1 \times 10^{-5}$	0.224	0.987	0.225	2.014

error observed from the pseudo-first-order model analysis further confirm that the process obeys the pseudo-first-order kinetics model perfectly.

### Sorption isotherm

The correlation which exists between the concentrations of BPA adsorbed and that at equilibrium were achieved using four adsorption isotherms. The Langmuir isotherm which predicts identical adsorption energies onto the surface can be described nonlinearly using Eq. 14 (Adeogun et al. 2011; Tewari and Kamaluddin 1998):

$$q_e = \frac{q_{\max} b C_e}{1 + b C_e} \quad (14)$$

The linear form is given as Eq. 15:

$$\frac{C_e}{q_e} = \frac{1}{q_{\max}} C_e + \frac{1}{b q_{\max}} \quad (15)$$

with  $q_e$  (mg/g) and  $C_e$  (mg/L) as previously discussed and the Langmuir constants ( $b$  (L/mg) and  $q_{\max}$  (mg/g)) estimated from the slope and intercept of the plot in Fig. 10a. The effectiveness of the sorption process was measured using the separation factor ( $R_L$ ) (Mohan et al. 2011). The expression for  $R_L$  is given as Eq. 16:

$$R_L = \frac{1}{1 + b C_e} \quad (16)$$

From Table 4, the value of  $R_L$  obtained is between 0 and 1 which indicates that the adsorption process is favorable (Mohsin et al. 2012). Moreso, the maximum monolayer coverage capacities ( $q_{\max}$ ) deduced from the Langmuir isotherm for the two sorbents were determined to be 115.85 mg/g and 166.67 mg/g for ACWS and MACWS, respectively. Table 5 presents favorable adsorption capacities of ACWS and MACWS adsorbents from this present study compared with various adsorbents for BPA removal reported in the literature.

The empirical equation proposed by Freundlich with given nonlinear form in Eq. 17 and linear form in Eq. 18 is represented in Fig. 10b (Freundlich 1907):

$$q_e = K_F C_e^{1/n} \quad (17)$$

$$\ln q_e = \ln K_F + \frac{1}{n} \ln C_e \quad (18)$$

where the Freundlich constants representing the relative adsorption capacity and the strength of sorption process are given as  $K_F$  (mg/g) and  $n$ , respectively. The extent of

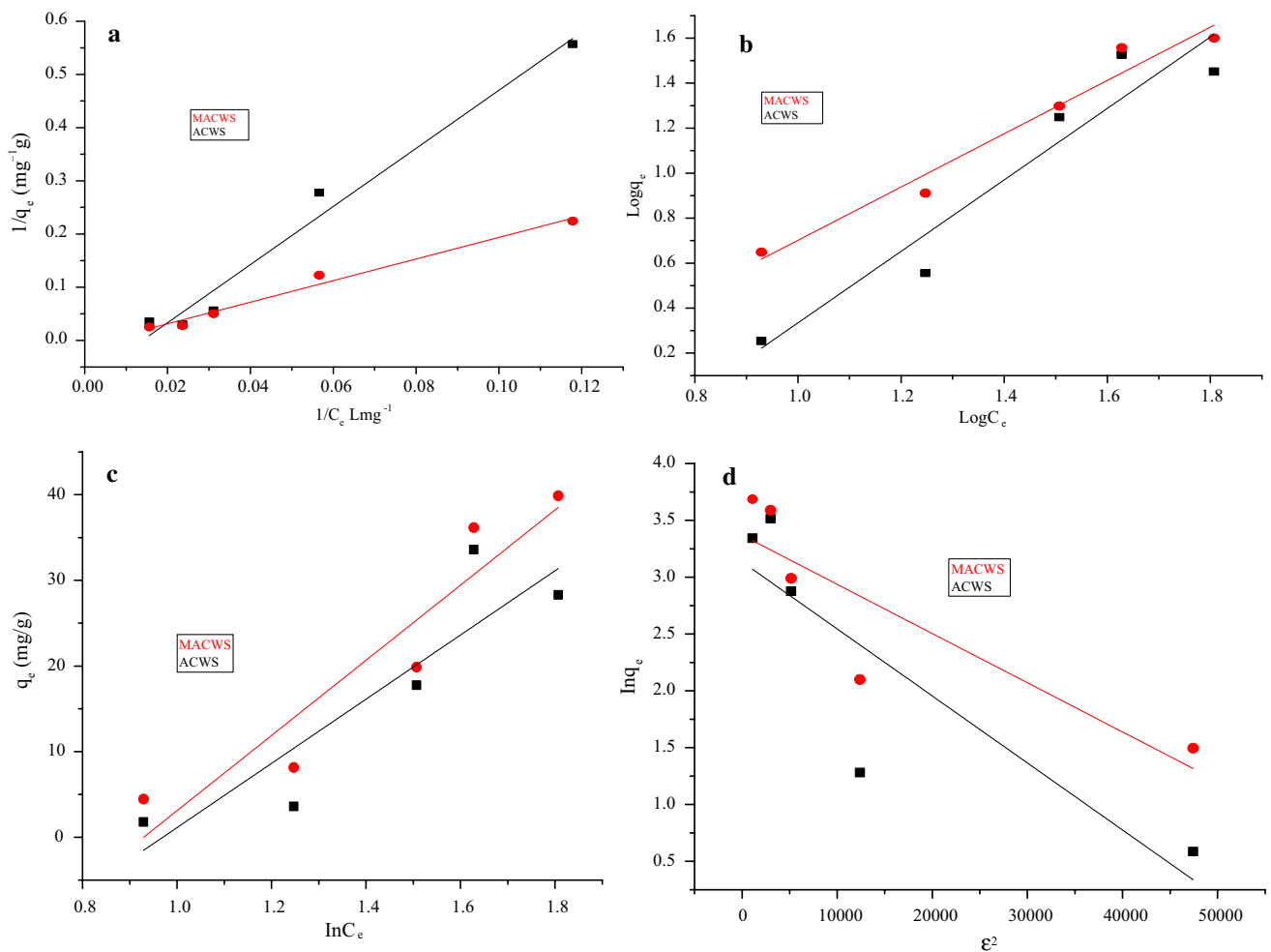


**Fig. 10** Plots of (a) Langmuir, (b) Freundlich, (c) Temkin and (d) Dubinin–Radushkevich isotherms for the adsorption of BPA unto ACWS–MACWS

**Table 5** Comparison of adsorption capacities of the two adsorbents used in this study with some other adsorbents for BPA adsorption

Adsorbents	$q_{max}$ (mg/g)	References
magnetite	4.78	Orimolade et al. (2018)
Mag-PVP <sup>a</sup>	115.87	Li et al. (2018)
CNTs/Fe <sub>3</sub> O <sub>4</sub> <sup>b</sup>	45.31	Li et al. (2015)
rGO-MNPs-3 <sup>c</sup>	106.40	Zhang et al. (2014)
Graphene oxide	87.80	Xu et al. (2013)
MMIPs <sup>d</sup>	142	Guo et al. (2011)
A-m-MWCNTs <sup>e</sup>	43.48	Bhatia and Dutta (2019)
Lignin	237	Han et al. (2012b)
ACWS	115.85	This study
MACWS	166.67	This study

<sup>a</sup>2-vinylpyridine functionalized magnetic nanoparticle  
<sup>b</sup>Carbon nanotubes grafted by magnetic Fe<sub>3</sub>O<sub>4</sub> particles  
<sup>c</sup>Reduced graphene oxide magnetic nanoparticles  
<sup>d</sup>Magnetic molecularly imprinted polymers  
<sup>e</sup>Aliquat 336-impregnated magnetic multiwalled carbon nanotubes

adsorption intensity or surface heterogeneity can be deduced from the slope with values between 0 and 1, and when its value gets closer to zero, it becomes more heterogeneous, whereas a value less than unity depicts chemisorption process (Adeogun et al. 2018). If  $n$  values are between 0 and 10, it is an indication of favorable sorption. As evident in the data presented in Table 4,  $1/n$  values for the two adsorbents were found to be 0.221 and 0.877, respectively, for ACWS and MACWS indicating that sorption of BPA unto the adsorbents is favorable ( $R^2 = 0.957$  and  $0.965$ ), respectively. However, this value is lower when compared to the  $R^2$  value from Langmuir isotherm. The Temkin isotherm explains the relationship that exists between adsorbent–adsorbate and presumes that the heat of adsorption of all molecules would reduce linearly and is given as Eq. 19:

$$q_e = \left(\frac{RT}{b}\right) \ln \alpha_\tau C_e \tag{19}$$

while the linear form is given as Eq. 20:

$$q_e = \left( \frac{RT}{b_T} \right) \ln \alpha_T + \frac{RT}{b_r} \ln C_e \quad (20)$$

where  $\alpha_T$ ,  $\alpha_r$  and  $b_T$  are the Temkin isotherm constants in L/g and  $\text{Jmol}^{-1}$ , and R and T are as previously defined. The plot is shown in Fig. 10c, and the values of  $\alpha_T$  determined are 2.397 and 2.117 L/mg for ACWS and MACWS, respectively, while  $b_T$  gave 345.53 and 336.58  $\text{Jmol}^{-1}$ , respectively, thus suggesting physical adsorption process, hence corroborating the report from kinetic study. The  $R^2$  was 0.929 and 0.942 for ACWS and MACWS, respectively, showing that Temkin does not totally fit the data compared to Langmuir and Freundlich. The nonlinear representation of the Dubinin–Radushkevich (DRK) isotherm is given as Eq. 21 (Gunnay et al. 2007; Dabrowski 2001):

$$q_e = q_s e^{-K_{ad} \epsilon^2} \quad (21)$$

while the linear form is given as Eq. 22:  $K_{ad}$

$$\ln q_e = \ln q_s - K_{ad} \epsilon^2 \quad (22)$$

where  $q_e$  and  $q_s$  are the amount adsorbed at equilibrium and the theoretical saturation capacity of the adsorbent in mg/g and mol/g, respectively,  $K_{ad}$  is DRK isotherm constant, and  $\epsilon$  is the Polanyi potential which can be estimated as Eq. 23:

$$\epsilon = R \ln \left( 1 + \frac{1}{C_e} \right) \quad (23)$$

The mean free energy, E ( $\text{kJmol}^{-1}$ ), was obtained as Eq. 24 (Dubinin 1960; Hobson 1969):

$$E = 1 / \sqrt{-2\beta} \quad (24)$$

The constant  $\beta$  is the mean free energy of adsorption per mol of the adsorbent ( $\text{mol}^2 \text{J}^{-2}$ ). The constants such as  $q_s$  and  $K_{ad}$  for the two adsorbents (ACWS and MACWS) were estimated using the plot in Fig. 10d, and their corresponding values were 10.585 and 12.613 mg/g and  $4 \times 10^{-5}$  and  $1 \times 10^{-5} \text{mol}^2 \text{kJ}^{-2}$ , respectively, while the mean free energy, E, values estimated to be 0.112 and 0.224  $\text{kJmol}^{-1}$ , respectively, points to a physisorption process since E is less than 8  $\text{kJmol}^{-1}$  (Santhi et al. 2009). The corresponding  $R^2$  values were 0.998 and 0.987, respectively, for ACWS and MACWS.

### Error function analysis

Two different error analyses functions were deployed in an attempt to further improve the fit of the adsorption equilibrium data to the various isotherms used in this study.

The hybrid fractional error function (HYBRID) is described as Eq. 25 (Rahdar et al., 2019; Ofudje et al., 2020):

$$\text{HYBRD} = \frac{100}{N - P} \sum_i^N \frac{(q_{(\text{exp})} - q_{(\text{cal})})}{q_{(\text{exp})}} \quad (25)$$

The root-mean-square error (RMSE) is given as Eq. 26 (Rahdar et al., 2019; Ofudje et al., 2020):

$$\text{RMSE} = \sqrt{\frac{\sum_i^N (q_{(\text{exp})} - q_{(\text{cal})})^2}{N}} \quad (26)$$

where the number of degrees of freedom of the system is given as N and the number of parameters as p. The experimental amount adsorbed and calculated amount adsorbed are  $q_{\text{exp}}$  and  $q_{\text{cal}}$  respectively. The results of the error functions of all the parameters compared revealed that the Langmuir model has lowest overall experimental error. Thus, it can be further affirmed that the Langmuir model best describes the experimental data and, thus, the best suited model in this present study.

### Statistical optimization analysis

To obtain proper regression equations, linear, two-factorial interaction (2FI), quadratic and cubic models were explored to evaluate the experimental data. In the same vein, sequential model sum of square coupled with model summary statistics was performed to establish the competence of these models in the removal of BPA by the two adsorbents used. The values of  $R^2$  validate the fitness of this model with higher value of  $R^2$  depicting better model in interpreting the experimental data, while F-test was used to certify the statistical significance (Peng et al. 2002). The results from the analysis of variance (ANOVA) in Tables 6 and 7 for BPA adsorption using ACWS and MACWS as adsorbents by quadratic model affirmed good relationship which exists between the response and the significant variables as described by the equation. If the value of F is large, while that of the probability (p) is small, then the more reliable is the corresponding coefficient term. According to Cobas et al. (2014), values of p lower than 0.05 certify a statistically significant model. The ANOVA (Table 6) reveals the F values as 5.13 and 9.89 for ACWS and MACWS, respectively, suggesting the applicability of the regression equation. In addition, the probability (p) value ( $p < 0.005$ ) for the adsorbents suggests that the model is significant.

Figures 11 and 12 present the combination effects of dosage, initial concentration, pH and temperature on the sorption of BPA by ACWS and MACWS, respectively. It was observed that greatest removal percentage was optimized at higher BPA concentration, temperature and dosage values. This was, however, contrary to what was observed in case of the effect of pH with greatest removal percentage in acidic range (lower pH values). This greater

**Table 6** ANOVA analysis of Box–Behnken model for BPA on ACWS adsorption factors

Source	Sum of squares	DF	Mean square	F value	Prob>F	
Model	1995.74	14	142.55	5.13	0.0021	significant
Dosage	538.05	1	538.05	19.35	0.0006	
Temperature	21.87	1	21.87	0.7867	0.3901	
Concentration	322.52	1	322.52	11.60	0.0043	
pH	129.34	1	129.34	4.65	0.0489	
Dosage × Temp	348.08	1	348.08	12.52	0.0033	
Dosage × Conc	8.08	1	8.08	0.2904	0.5984	
Dosage × pH	155.39	1	155.39	5.59	0.0331	
Temp. × Conc	55.31	1	55.31	1.99	0.1802	
Temp. × pH	28.02	1	28.02	1.01	0.3325	
Conc. × pH	32.10	1	32.10	1.15	0.3008	
(Dosage) <sup>2</sup>	261.48	1	261.48	9.40	0.0084	
(Temp.) <sup>2</sup>	31.44	1	31.44	1.13	0.3056	
(Conc.) <sup>2</sup>	5.23	1	5.23	0.1882	0.6710	
pH <sup>2</sup>	94.15	1	94.15	3.39	0.0870	
Residual	389.26	14	27.80			
Lack of Fit	336.97	10	33.70	2.58	0.1874	Not significant
Pure Error	52.29	4	13.07			
Cor Total	2385.00	28				

**Table 7** ANOVA analysis of Box–Behnken model for BPA on MACWS adsorption factors

Source	Sum of squares	DF	Mean square	F value	Prob>F	
Model	2373.27		169.52	9.89	<0.0001	Significant
Dosage	1548.71	1	1548.71	90.31	<0.0001	
Temperature	117.03	1	117.03	6.82	0.0205	
Concentration	162.67	1	162.67	9.49	0.0082	
pH	283.40	1	283.40	16.53	0.0012	
(Dosage) <sup>2</sup>	11.95	1	11.95	0.70	0.4179	
(Temperature) <sup>2</sup>	7.62	1	7.62	0.44	0.5158	
(Concentration) <sup>2</sup>	3.07	1	3.07	0.18	0.6784	
(pH) <sup>2</sup>	8.75	1	8.75	0.51	0.4869	
Dosage × Temp	42.52	1	42.52	2.48	0.1377	
Dosage × Conc	76.10	1	76.10	4.44	0.0537	
Dosage × pH	33.60	1	33.60	1.96	0.1834	
Temp × Conc	20.04	1	20.04	1.17	0.2980	
Temp × pH	66.70	1	66.70	3.89	0.0687	
Conc. × pH	1.57	1	1.57	0.091	0.7668	
Residual	240.08	14	17.15			
Lack of fit	215.44	10	21.54	3.50	0.1194	Not significant
Pure Error	24.63	4	6.16			
Cor Total	2613.35	28				

sorption percentage at acid pH range may be as a result of the electrostatic interaction that exists between the surface of the adsorbents which is positively charged and the negative charge of the bisphenol structure. Also, the increase in the sorption percentage of BPA with the adsorbents is due to the increase in the surface area available

for sorption which thus increases the adsorption receptors for the removal of the contaminants. It was deduced further that magnetic treatment of the walnut shell greatly enhanced the removal ability of the adsorbent, thus boosting the adsorption process. Similar report was documented before by de Sales et al. 2013.

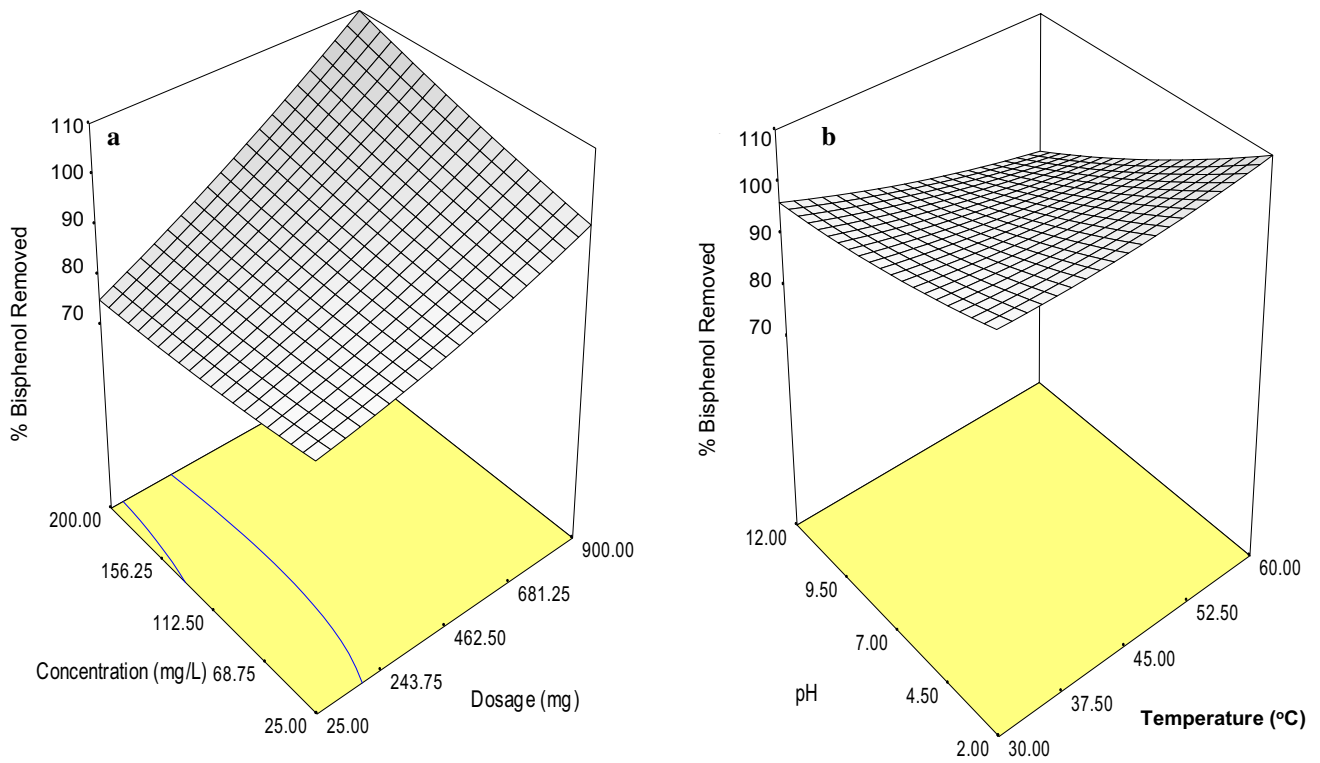


**Fig. 11** Response surface 3-D plots for the removal efficiency of BPA onto ACWS showing effects of (a) initial concentration and dosage and (b) pH and temperature

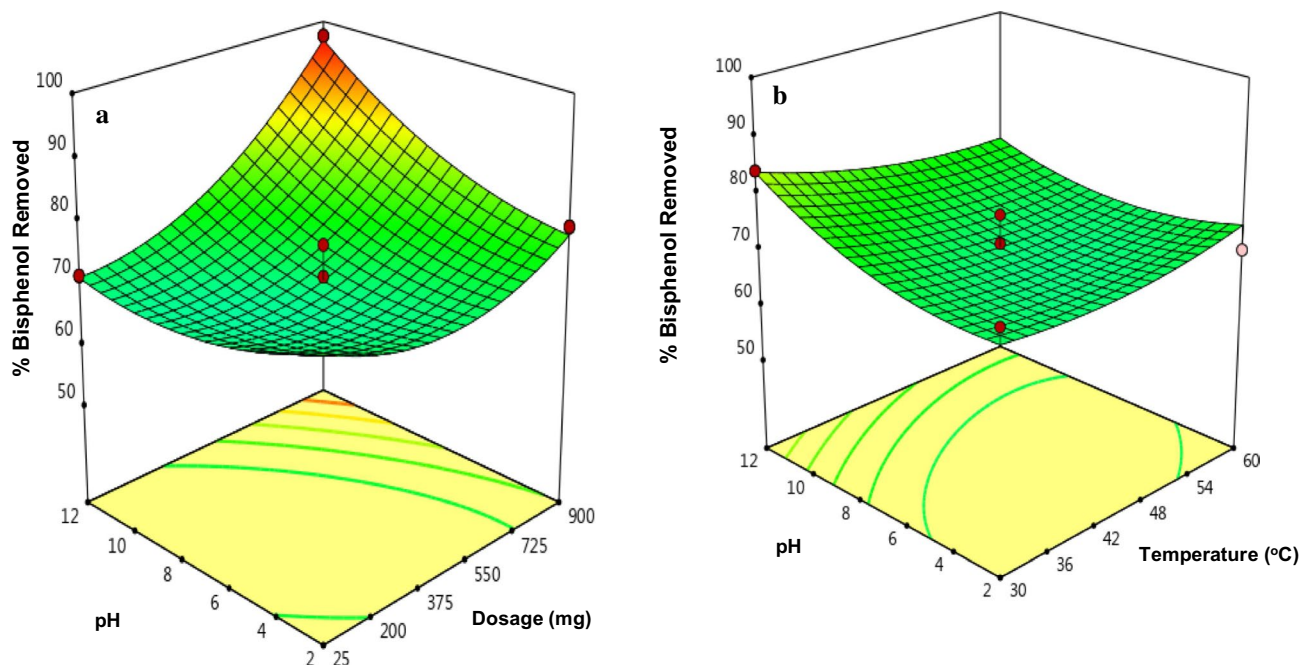


**Fig. 12** Response surface 3-D plots for the removal efficiency of BPA onto MACWS effects of (a) pH and dosage and (b) pH and temperature

## Conclusion

The work assessed the use of activated carbon prepared from walnut shells and its magnetized counterpart as adsorbents in the adsorption of BPA from aqueous solution. It was observed that the uptake of BPA on ACWS and MACWS decreased with increased pH, while the adsorption capacity increased as the adsorbent dosage and BPA concentration increased for the two adsorbents. The adsorption process followed pseudo-first-order model. The equilibrium data were well explained by the Langmuir isotherm model implying monolayer formation. The thermodynamic parameters revealed that the adsorption process is spontaneous and endothermic in nature. From the FT-IR investigation, carboxylate and phenolic functional groups could be associated with the adsorption process as evident from the changes in the IR bands.

**Acknowledgements** The contributions of staff from Central Research Laboratory and Department of Chemistry, Federal University of Agriculture, Abeokuta, Nigeria, are well appreciated. The efforts of the technical staff of CSIR-CECRI, India, for the characterization are appreciated.

**Authors' contributions** Not Applicable.

**Funding** This research did not receive any specific grant from funding agencies in the public, commercial or not-for-profit sectors.

**Availability of data and material** Not Applicable.

**Code availability** Not Applicable.

## Declarations

**Conflict of interest** Authors declare that there are no conflicts of interest.

**Open Access** This article is licensed under a Creative Commons Attribution 4.0 International License, which permits use, sharing, adaptation, distribution and reproduction in any medium or format, as long as you give appropriate credit to the original author(s) and the source, provide a link to the Creative Commons licence, and indicate if changes were made. The images or other third party material in this article are included in the article's Creative Commons licence, unless indicated otherwise in a credit line to the material. If material is not included in the article's Creative Commons licence and your intended use is not permitted by statutory regulation or exceeds the permitted use, you will need to obtain permission directly from the copyright holder. To view a copy of this licence, visit <http://creativecommons.org/licenses/by/4.0/>.

## References

- Adeogun AI, Ofudje EA, Idowu MA, Kareem SO (2011) Equilibrium, kinetic and thermodynamic studies of the biosorption of Mn (II) ions from aqueous solute and acid-treated corncob. *BioResources* 6(4):4117–4134
- Adeogun AI, Ofudje EA, Idowu MA, Kareem SO, Vahidhabanu S, Babu BR (2018) Biosorption of Cd<sup>2+</sup> and Zn<sup>2+</sup> from aqueous solution using tilapia fish scale (*Oreochromis* sp): Kinetics, isothermal and thermodynamic study. *Desalin Water Treat* 107:182–194
- Ahmedna M, Marshall WE, Husseiny AA, Rao RM, Goktepe I (2004) The use of nutshell carbons in drinking water filters for removal of trace metals. *Water Res* 38:1062–1068
- Akande IS, Hassan O, Adeshakin A (2013) Gas Chromatography-mass spectrophotometry evaluation of the concentration of Bisphenol-A (BPA) in Five selected canned food products consumed in lagos area, Nigeria. *Br J Appl Sci Technol* 4(1):187–197
- Al-qodah Z (2000) Adsorption of dyes using shale oil ash. *Water Resour* 34:429–4303
- Balci B, Erkurt FE (2017) Adsorption of Bisphenol-A by eucalyptus bark/magnetite composite: modeling the effect of some independent parameters by multiple linear regression. *Adsorpt Sci Technol* 35(3–4):339–356
- Bhatia D, Datta D (2019) Removal of bisphenol-a using amine-modified magnetic multiwalled carbon nanotubes: batch and column studies. *J Chem Eng Data* 64(6):2877–2887
- Cobas M, Sanroman M, Pazos M (2014) Box-Behnken methodology for Cr VI and leather dyes removal by an eco-friendly biosorbent: vesiculosus. *Bioresour Technol* 160:164–174
- Dabrowski A (2001) Adsorption-from theory to practice. *Adv Colloid Interface Sci* 93:135–224
- Dang VBH, Doan HD, Dang-Vu T, Lohi A (2009) Equilibrium and kinetics of biosorption of cadmium II and copper II ions by wheat straw. *Biores Technol* 100:211–219
- de Sales PF, Magriotis ZM, Rossi MALS, Resende RF, Nunes CA (2013) Optimization by response surface methodology of the adsorption of coomassie blue dye on natural and acid-treated clays. *J Environ Manage* 130:417–428
- Dubinin MM (1960) The potential theory of adsorption of gases and vapors for adsorbents with energetically non-uniform surface. *Chem Rev* 60:235–266
- Freundlich H (1907) Uber die adsorption in Losungen. *Z Phys Chem* 57U:385–470
- Gbasemian E, Vatanara A, Najafabadi AR, Rouini MR, Gilani K, Darabi M (2013) Preparation, characterization and optimization of sildenafil citrate loaded PLGA nanoparticles by statistical factorial design. *DARU J Pharm Sci* 21(68):1–10
- Gunnay A, Arslankaya E, Tosun I (2007) Lead removal from aqueous solution by natural and pretreated clinoptololite: adsorption equilibrium and kinetics. *J Hazard Mater* 146:362–371
- Guo W, Hu W, Pan J, Zhou H, Guan W, Wang X, Dai J, Xu L (2011) Selective adsorption and separation of BPA from aqueous solution using novel molecularly imprinted polymers based on kaolinite/Fe<sub>3</sub>O<sub>4</sub> composites. *Chem Eng J* 171:603–611
- Han W, Luo L, Zhang S (2012b) Adsorption of bisphenol a on lignin: effects of solution chemistry. *Int J Environ Sci Technol* 9:543–548
- Himanshu P, Vashi RT (2010) A study on the removal of toluidine blue dye from aqueous solution by adsorption onto neem leaf powder. *Inter Scholarly and Sci Resear Innov* 4:674–679
- Ho YS (2004) Citation review of Lagergren kinetic rate equation on adsorption reactions. *Scientometrics* 59:171–177
- Hobson JP (1969) Physical adsorption isotherms extending from ultra-high vacuum to vapour pressure. *J Phys Chem* 73:2720–2727
- Li S, Gong Y, Yang Y, He C, Hua L, Zhu L, Sun L, Shu D (2015) Recyclable CNTs/Fe<sub>3</sub>O<sub>4</sub> magnetic nanocomposites as adsorbents to remove bisphenol A from water and their regeneration. *Chem Eng J* 260:31–239
- Li Q, Pan F, Li W, Li D, Haiming X, Xia D, Li A (2018) Enhanced adsorption of bisphenol a from aqueous solution with

- 2-vinylpyridine functionalized magnetic nanoparticles. *Polymers* 10(10):1136. <https://doi.org/10.3390/polym10101136>
- Manzato L, Takeno ML, Pessoa-Junior WAG, Mariuba LAM, Simonsen J (2018) Optimization of cellulose extraction from jute fiber by box-behken design. *Fibers Polym* 19:289–296
- Mohan D, Sarswat A, Singh VK, Alexandre-Franco M, Pitman CU Jr (2011) Development of magnetic activated carbon from almond shells for trinitrophenol removal from water. *Chem Eng J* 172:1111–1125
- Mohsin K, Nadeem F, Hassan J, Mohammad Z (2012) Biosorption of copper II on dry product: characterization, kinetics and equilibrium studies. *J Chem Soc Pakistan* 34(6):1356–1365
- Ofudje EA, Awotula AO, Hambate GV, Akinwunmi F, Alayande SO, Olukanni OD (2017) Acid activation of groundnut husk for copper adsorption: kinetics and equilibrium studies. *Desalin Water Treat* 86:240–251
- Ofudje EA, Adeogun IA, Idowu MA, Kareem SO, Ndukwe NA (2020) Simultaneous removals of cadmium(II) ions and reactive yellow 4 dye from aqueous solution by bone meal-derived apatite: kinetics, equilibrium and thermodynamic evaluations. *J Anal Sci Technol*. <https://doi.org/10.1186/s40543-020-0206-0>
- Orimolade BO, Adekola FA, Adebayo GB (2018) Adsorptive removal of bisphenol A using synthesized magnetite nanoparticles. *Appl Water Sci*. <https://doi.org/10.1007/s13201-018-0685-y>
- Peng L, Xu X, Mu H, Hoy CE, Alder-Nissen J (2002) Production of structured phospholipids by lipase-catalyzed acidolysis: optimization using response surface methodology. *Enzyme Microb Technol* 31:523–532
- Pivnenko K, Pedersen GA, Eriksson E, Astrup TF (2015) Bisphenol A and its structural analogues in household waste paper. *Waste Manage* 44:39–47
- Qiu P, Cui M, Kang K, Park B, Son Y, Khim E, Jang M, Khim J (2014) Application of box-behken design with response surface methodology for modeling and optimizing ultrasonic oxidation of arsenite with H<sub>2</sub>O<sub>2</sub>. *Cent Eur J Chem* 12(2):164–172
- Riry W, Tony H, Abdull RMY, Zulkifli Y (2014) Removal of bisphenol A from aqueous solution by activated carbon derived from oil palm empty fruit bunch. *Water Air Soil Pollut* 225(2148):1–12
- Santhi T, Manonmani S, Smitha T, Mahalakshmi K (2009) Adsorption of malachite green from aqueous solution onto a waste aqua cultural shell powders Prawn waste: kinetic study. *Rasayan J Chem* 24:813–824
- Tewari BB, Kamaluddin MD (1998) Interaction of 2,4-dinitrophenol and 2,4,6-trinitrophenol with copper, zinc, molybdenum and chromium ferrocyanides. *Colloids Surf, A* 131:89–93
- Upendra K (2011) Thermodynamics of the adsorption of Cd II from aqueous solution on NCRH cylinder. *Int J Environ Sci Develop* 2:334–336
- vom Saal FS, Hughes C (2006) Bisphenol-A- vom saal and hughes respond. *Environ Health Perspect* 114(1):a16–a21
- Xu J, Zhu Y (2013) Elimination of bisphenol A from water via graphene oxide adsorption. *Acta Phys Chim Sin* 29(4):829–836
- Zhang Y, Cheng Y, Chen N, Zhou Y, Li B, Gu W, Shi X, Xian Y (2014) Recyclable removal of bisphenol A from aqueous solution by reduced graphene oxide–magnetic nanoparticles: adsorption and desorption. *J Colloid Interface Sci* 421:85–92
- Zhou Q, Wang Y, Xiao J, Fan H (2016) Adsorption and removal of bisphenol A,  $\alpha$ -naphthol and  $\beta$ -naphthol from aqueous solution by Fe<sub>3</sub>O<sub>4</sub>@polyaniline core–shell nanomaterials. *Synth Met* 212:113–122
- Zhou Y, Hu Y, Huang W, Cheng G, Cui C, Lu J (2018) A novel amphoteric  $\beta$ -cyclodextrin based adsorbent for simultaneous removal of cationic/anionic dyes and bisphenol A. *Chem Eng J* 341:47–57
- Han KL, Tjoon TT, Mohamad HI, Anees A, Hui TC (2012a) Adsorption and Removal of Zinc II from Aqueous Solution Using Powdered Fish Bones. *APCBEE Procedia* 96–102

**Publisher's Note** Springer Nature remains neutral with regard to jurisdictional claims in published maps and institutional affiliations.